



## Variable numbers of calreticulin genes in *Trypanosoma cruzi* correlate with atypical morphology and protein expression

Andrea González<sup>a</sup>, Steffen Härtel<sup>b</sup>, Jorge Mansilla<sup>b</sup>, Fernando Sánchez-Valdéz<sup>c,\*</sup>, Arturo Ferreira<sup>a,\*\*</sup>

<sup>a</sup> Laboratorio de Inmunología de la Agresión Microbiana, Programa Disciplinario de Inmunología, Instituto de Ciencias Biomédicas, Facultad de Medicina, Universidad de Chile, Chile

<sup>b</sup> Laboratorio de Análisis de Imágenes Científicas (SCIAN-lab), Instituto de Neurociencias Biomédica (BNI), Instituto de Ciencias Biomédicas (ICBM), Facultad de Medicina, Universidad de Chile, Chile

<sup>c</sup> Instituto de Patología Experimental- CONICET, Universidad Nacional de Salta, Salta, Argentina

### ARTICLE INFO

#### Keywords:

*Trypanosoma cruzi*  
Calreticulin  
Genetically modified parasites

### ABSTRACT

*Trypanosoma cruzi* calreticulin (TcCalr, formerly known as TcCRT), upon binding to Complement (C) C1 and ficolins, inhibits the classical and lectin pathways and promotes infectivity. This virulence correlates with the expression of TcCalr. The TcCalr C inhibitory capacity was shown in a previous work using a clonal epimastigote cell line from the TCC *T. cruzi* strain, lacking one TcCalr allele (*TcCalr* +/−) or over expressing it (*TcCalr* +). In this work, we detected atypical morphology in *TcCalr* +/− and in *TcCalr* + parasites, as compared to the wild-type (WT) strain. Polyclonal anti-TcCalr antibodies detected TcCalr presence mainly in the parasite nucleus. The number of TcCalr indicator gold particles, detected in electron microscopy and quantified *in silico*, correlated with the number of TcCalr coding genes. Both *TcCalr* + and *TcCalr* +/− epimastigotes presented morphological alterations.

### 1. Introduction

Chagas disease is now a worldwide problem. Current treatment includes the use of Nifurtimox and Benznidazole, with severe side effects and treatment failure, mainly in the chronic stage (Clayton, 2010). Thus, novel therapies are required. *Trypanosoma cruzi* (the agent of Chagas disease) has at least three known stages during its life cycle: infective trypomastigotes, non-infective epimastigotes and intracellular amastigotes. To maintain this cycle and consequently, its survival, the parasite uses multiple strategies to evade the host immune system. One of its major virulence factors is *Trypanosoma cruzi* calreticulin (TcCalr, formerly known as TcCRT) (Ramírez et al., 2011), a 47-kDa lectin chaperone. In spite of having an endoplasmic reticulum (ER)-retention signal KEDL, on the carboxyl-terminal domain (Ferreira et al., 2004a), TcCalr is found in different organelles in free and intracellular parasites, including Golgi, nucleus, kinetoplast, and cytoplasm (Gonzalez et al., 2015; Souto-Padron et al., 2004).

TcCalr is also translocated from the ER, mainly to the area of flagellum emergence (Ferreira et al., 2004b) where, through its central S domain, interacts with C1, thus inhibiting the early stages of the

complement (C) classical pathway (Ferreira et al., 2004b; Valck et al., 2010; Ramirez-Toloza and Ferreira, 2017). Inactive C1 remains bound to the parasite, thus mediating its interaction with host cell calreticulin (CALR) (Ramírez et al., 2011, 2012). TcCalr can also inhibit the C lectin pathway through its interaction with L-Ficolin (Sosoniuk et al., 2014). Thus, these properties allow TcCalr to act as a main virulence factor. Through a different domain, located in the amino terminal sequences, extracellular TcCalr interacts with endothelial cells (ECs), possibly through a Scavenger-Receptor class A with collagenous structure, since this interaction is inhibited by fucoidan, a homopolymer of sulphated L-fucose (Lopez et al., 2010), which is a known pharmacological inhibitor of this receptors. The interaction with ECs may also occur, *via* C1, with CALR exteriorized by these cells (Ferreira et al., 2004b). Moreover, TcCalr interaction with ECs mediates anti-angiogenic and anti-tumour effects (Lopez et al., 2010; Molina et al., 2005; Ferreira et al., 2005; Ramirez-Toloza et al., 2016).

By electron microscopy, we have previously described the topographical localization of TcCalr in intracellular trypomastigotes, free trypomastigotes and non-infective epimastigotes (González et al., 2015). Notable differences between trypomastigotes and epimastigotes

\* Corresponding author at: Independencia 1027, Independencia, Santiago, Chile.

\*\* Corresponding author at: Avenida Bolivia 5150, Salta, Argentina.

E-mail addresses: [ipe.unsa@gmail.com](mailto:ipe.unsa@gmail.com) (F. Sánchez-Valdéz), [afferreir@med.uchile.cl](mailto:afferreir@med.uchile.cl) (A. Ferreira).

were detected. Herein, as a first aim, we compare the morphological differences between *T. cruzi* epimastigotes, a non-infective parasite form, genetically modified in their capacity to express TcCalr: *TcCalr* + epimastigotes that over express the protein, and *TcCalr* +/- epimastigotes that lacks one *TcCalr* allele. TcCalr was localized *in situ* in these parasites, and then quantified by *in silico* means. This is the first report on TcCalr localization in genetically modified parasites and associated morphological consequences.

While trypomastigotes are inside the mammalian cell, TcCalr is found mainly in kinetoplast and nucleus (Gonzalez et al., 2015), suggesting a secretor pathway, with kinetoplasts representing a stopover, where TcCalr accumulates, before TcCalr translocation to the parasite membrane. In non-infective epimastigotes, TcCalr is only marginally translocated (Sosoniuk et al., 2014). TcCalr rather locates mainly in the epimastigote nucleus (Gonzalez et al., 2015). These facts are probably relevant to explain the main differences between these infective and non-infective parasite forms, especially with regard to C susceptibility and C-mediated infectivity (Ramirez et al., 2011; Sanchez-Valdez et al., 2013). Moreover, *T. cruzi* epimastigotes with exogenously attached TcCalr present increased infectivity (Sosoniuk-Roche et al., 2017).

*TcCalr*+ epimastigotes display increased survival capacity in the presence of human C, as well as enhanced *in vivo* infectivity, when compared to the *TcCalr* WT and *TcCalr* +/- parasites (*TcCalr* null mutant parasites are not viable, given the central relevance of this chaperone in parasite physiology) (Sanchez Valdez et al., 2013; Sanchez-Valdez et al., 2014). However, how this genetic modification affects the parasite morphology is unknown, and this is a second aim of this work.

## 2. Materials and methods

### 2.1. Genetically modified TCC + and TCC +/- parasites generation

Genetically modified parasites were produced as described (Sanchez-Valdez et al., 2013). In brief, for *TcCalr* +/- strain, electroporation with a recombination fragment was performed with a pTREC empty construction, designed using the Gateway cloning System, that allows the complete replacement of the *TcCalr* gene in one allele. For the *TcCalr*+ strain, the complete *TcCalr* coding sequence was cloned into the pTREC plasmid was performed, and then electroporated into the WT parasite. The transfection was performed using TCC log phase epimastigotes.

### 2.2. Transmission electron microscopy (TEM)

Performed as previously described (Gonzalez et al., 2015).  $10^8$  *TcCalr* +/-, WT and *TcCalr*+ epimastigotes were harvested, washed twice with phosphate-buffered saline (PBS) (NaCl 137 mM, KCl 2.7 mM,  $\text{Na}_2\text{HPO}_4$  10 mM,  $\text{KH}_2\text{PO}_4$  1.8 mM, pH 7.4) and fixed in glutaraldehyde 3% v/v, o.n at 4 °C. Then they were washed and post-fixed with osmium tetroxide 1% v/v in phosphate buffer (sodium phosphate 0.1 M, pH 7.3). Samples were rinsed and progressively dehydrated in ethanol from 30% to absolute. Then they are treated with acetone and finally embedded in EPON at 70 °C. Ultrathin sections (700 Å) were placed on copper grids, stained with 5% (w/v) aqueous uranyl acetate and lead citrate and then observed in electron microscope (Zeiss EM-109), at 80 kV.

### 2.3. Immunocytochemistry

Performed as previously described (Gonzalez et al., 2015). Basically,  $10^8$  *TcCalr* +/-, WT and *TcCalr*+ epimastigotes were fixed in 4% paraformaldehyde and 0.1% glutaraldehyde in cacodylate buffer 0.1 M (pH 7.2) overnight at 4 °C. Free aldehyde groups were blocked with 50 mM ammonium chloride. Samples were rinsed and sequentially dehydrated in 30% to absolute ethanol, at room temperature and

embedded in a modified epoxic resin: Polybed (Electron Microscopy Science) at 60 °C. Ultrathin sections of 700 Å were obtained, collected on nickel grids, and, after immunocytochemical procedures, were stained with 5% (w/v) aqueous uranyl acetate, and then observed in Zeiss EM-109 and in Phillips-TECNAI 12 electron microscopes, both at 80 kV.

### 2.4. Immunocytochemical procedures for TcCalr detection

As previously described (Gonzalez et al., 2015), nickel grids containing sections of 700 Å were floated, for 30 min at room temperature, in TRIS 0.02 M pH 7.2 containing 0.02% sodium azide, 0.15 M sodium chloride, 0.1% bovine serum albumin, and 0.05% Triton X-100 (BuFi). Then, the sections were incubated o.n at 4 °C with a primary antibody (Polyclonal antiserum anti-TcCRT 1/32,000 v/v) diluted in BuFi. After washing in BuFi, sections were incubated for 2 h with a secondary antibody (Goat anti-rabbit IgG conjugated to colloidal gold, 10 nm; Sigma G7402) diluted 1/20 in BuFi, prior centrifugation for 10 min at 6000 rpm. After washing, the sections were rinsed with deionized water. Controls include sections incubated with secondary antibody and preimmune serum.

### 2.5. Quantification of label density generated by polyclonal antibodies

Gold particles/ $\mu\text{m}^2$  in epimastigotes were quantified as previously described (Gonzalez et al., 2015) using Image analysis routines (SCIAN-Soft) based on Interactive Data Language IDL 7.1 (ITT, Boulder, CO).

### 2.6. Morphological analysis

Analysis of structure was performed using a double-blind analysis of microphotographs with an electron microscopy expert. Criteria for evaluation used a WT epimastigote microphotograph from previous studies (Gonzalez et al., 2015) and evaluated a) shape, b) nuclei structure, c) External membrane integrity. All microphotographs were analyzed by number and then classified by the condition. To standardize after the analysis 6 microphotographs per condition were chosen to perform the percentage and statistics.

### 2.7. Statistical analysis

Results for morphological analysis are expressed as percentage of parasites with visible alterations in a double-blind analysis. Results of quantification of gold particles are expressed in number of particles/ $\mu\text{m}^2$ . Both data were evaluated using Graphpad Prism v.5 and significant differences were obtained using a two-way ANOVA (morphology) and a one-way ANOVA (quantification). Significance was taken at  $p < 0.05$ .

## 3. Results

### 3.1. TcCalr expression in situ correlates with the genetic modification in TCC epimastigotes

*TcCalr*+ epimastigotes had more TcCalr molecules per  $\mu\text{m}^2$  than WT epimastigotes, which, in turn, had more TcCalr molecules per  $\mu\text{m}^2$  than *TcCalr* +/- epimastigotes (Fig. 1), indicating that the *in situ* quantification of TcCalr number reflects the number of active TcCalr coding genes, as previously determined (Sanchez-Valdez et al., 2013).

### 3.2. Genetically modified parasites present altered morphology

Morphological studies showed that 83% of *TcCalr* +/- (Fig. 2A) and 50% of *TcCalr*+ (Fig. 2C) epimastigotes present loss of the elongated characteristic form, when compared to the WT counterpart (Fig. 2B), where 12.5% showed these alterations. Furthermore, nuclei

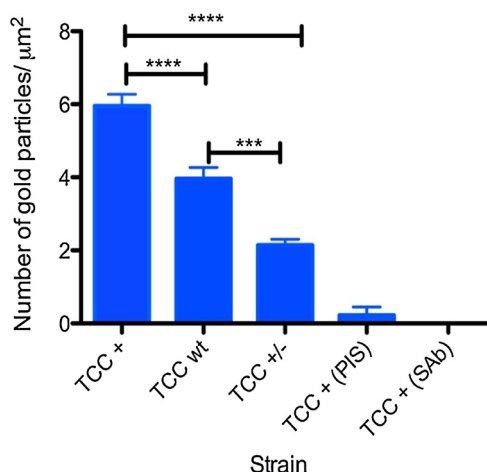


**Fig. 1.** TcCalr expression correlates with the number of coding genes. TcCalr + epimastigotes displayed more gold particles than TcCalr WT parasites. In turn, TcCalr WT had more gold particles than TcCalr +/- epimastigotes, consistent with the genetic modification performed. The TCC + strain was employed as control with pre-immune serum (PIS) and only with secondary antibody (SAb) (right columns). Bars show mean values from N = 6 microphotographs. Error bars are standard deviations. Statistical analysis was performed with a One-way ANOVA (\*\*\* = p < 0.01, \*\*\*\* = p < 0.001).

structure was altered in 100% of the *TcCalr* +/- and 83% of the *TcCalr* +, compared to the 38% of the WT counterpart. In addition, the external membrane was less defined in 100% of the *TcCalr* +/- and 67% of the *TcCalr* +, as compared to the 38% of the WT and to what is observed in a previous work (Gonzalez et al., 2015). These results are summarized in Fig. 2D. Moreover, in the *TcCalr* +/- sample, the parasite shown is probably undergoing cell division, but only one nucleus is poorly visible (Fig. 2A). In the *TcCalr* + sample only a large dense reservosome can be identified (Fig. 2C). Schematic representation of the *T. cruzi* morphology and principal alterations upon genetic modification, is shown on Fig. 3.

### 3.3. Genetically modified parasites *TcCalr* is located mainly in the parasite nucleus

The *TcCalr in situ* detection showed that the nucleus was its main sub cellular localization in all samples, a fact consistent with previous studies (Gonzalez et al., 2015). However, some particles can be observed in other organelles such as cytoplasm (Fig. 4). 66% of *TcCalr* + epimastigotes (Fig. 4C) presented more gold particles than the WT (Fig. 4B) and the *TcCalr* +/- (Fig. 4A) samples, as determined by direct observation of the microphotographs. As expected, no particles were detected in controls incubated with a pre-immune serum (Fig. 4D) or with just the secondary-gold labelled antibody (Fig. 4E) (Each picture represents about 1/30<sup>th</sup> of the total parasite).

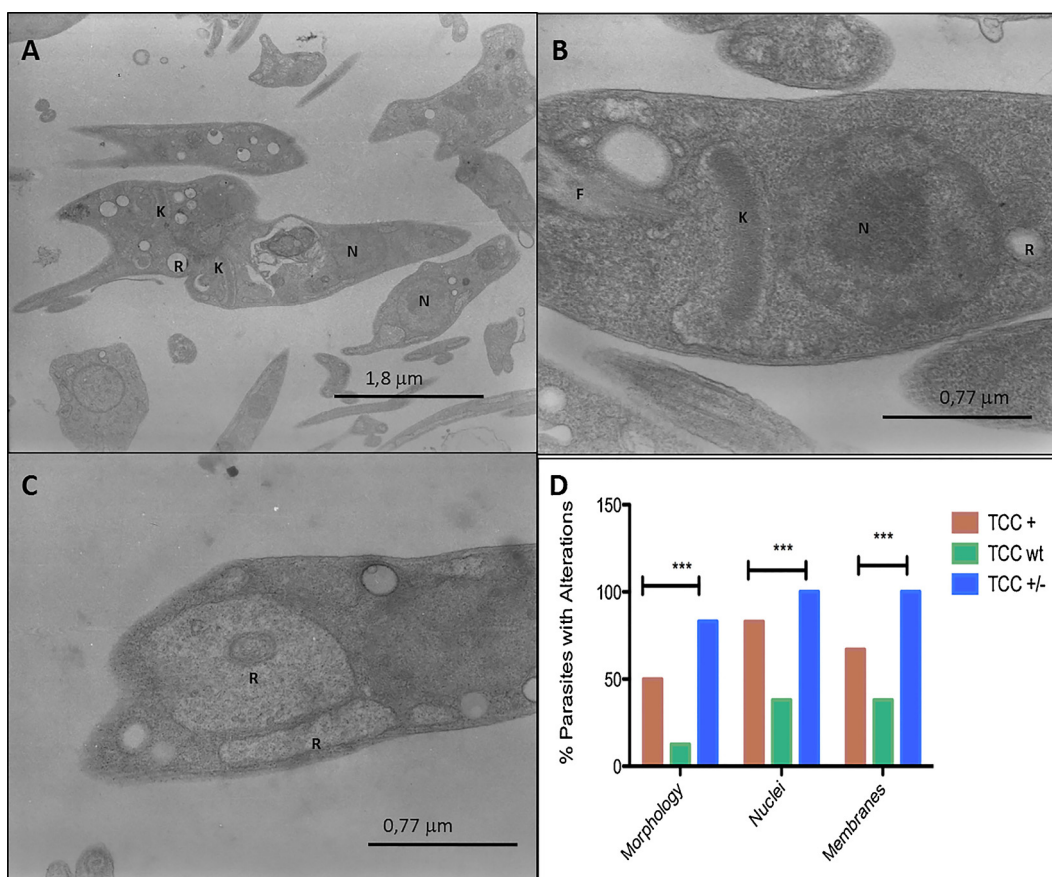


**Fig. 2.** Genetically modified parasites are morphologically altered. A. *TcCalr* +/- epimastigotes (20,000X), abnormal structure is observed with several numbers of reservosomes (R); B. *TcCalr* WT epimastigotes (30,000X), present well-defined organelles and ultra structure; C. *TcCalr* + epimastigotes (30,000X) present an abnormal swelling of reservosomes (R). D. Summary of the percentage of parasites with altered organelles. Genetically modified parasites present significantly more altered organelles than the wt counterpart. Statistical analysis was performed with a Two-way ANOVA analysis, \*\*\* = p < 0.003. Bars: Standard deviations. K: Kinetoplast, F: Flagellum, N: Parasite nucleus, R: Reservosome. Electron microphotographs are representative of a set of 6 photos per condition, for a double blind morphological analysis.

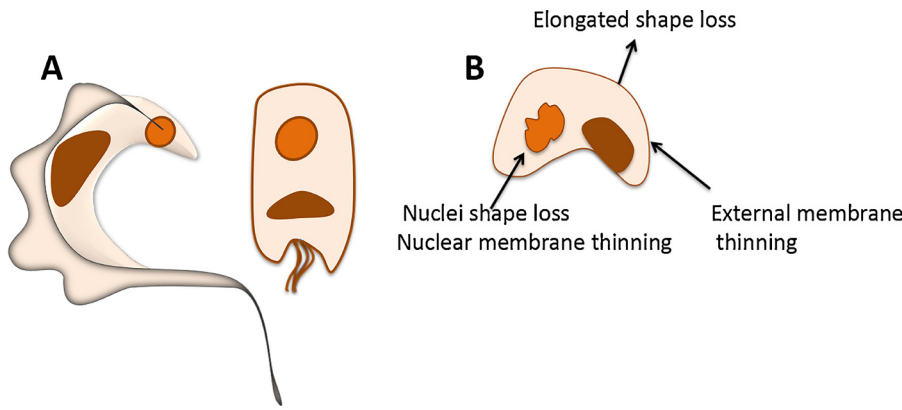


**Fig. 3.** Schematic representation of *T. cruzi* morphology in normal and genetically modified parasites. A. Normal parasite: Elongated form, a well-defined spherical nucleus with normal external and nuclear membranes. B. Genetically modified parasites: Thinning of external and nuclear membrane. Normal elongated parasite shape and rounded nucleus are also altered.

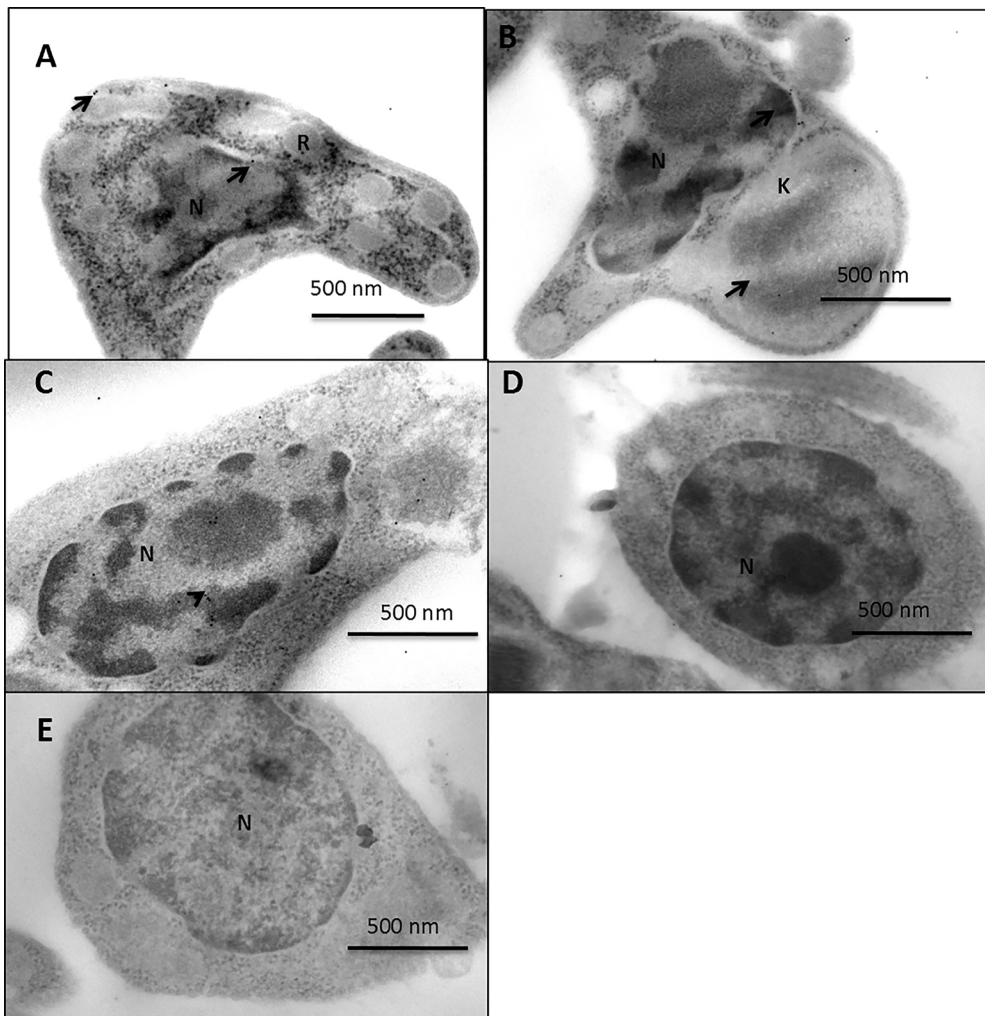


**Fig. 4.** Calreticulin is differentially detected in genetically modified parasites, particularly in nucleus. Gold particles were detected in: A. *TcCalr* +/-, in the nucleus (N), reservosome (R), and cytoplasm (C). B. *TcCalr* WT, in the nucleus (N), and kinetoplast (K). It can also be observed a few particles outside the parasites, in the resin. C. *TcCalr* + sample (30,000X), mainly in nucleus (N). D–E. *TcCalr* + control samples. No gold particles were observed. A–C: Anti-r*TcCalr* PoAb, 1/32,000 v/v; D. Pre-immune serum 1/32,000 v/v; E. Anti-rabbit IgG conjugated to colloidal gold (10 nm), 1/20 v/v. K: Kinetoplast, F: Flagellum, N: Parasite nucleus, R: Reservosome. Arrows: Positive signals. All samples are 30,000×. Electron microphotographs are representative of a set of 6 photos per condition.

**4. Discussion**

The *TcCalr* +/- strain present several interesting features leading to additional experimental studies of its potential protective immunogenic properties (Sanchez-Valdez et al., 2014, 2015). In a previous work, the *TcCalr*+ strain was more resistant to complement mediated lysis when compared to the WT or the *TcCalr*+/- counterpart (Sanchez-Valdez et al., 2013). However, infection with *TcCalr* +/- induced less anti-*TcCalr* antibodies in Balb/c mice than the WT or *TcCalr*+ counterpart (Sanchez-Valdez et al., 2014). Thus, protection of Balb/c mice with the *TcCalr* +/- strain seems to be antibody-

independent (Sanchez-Valdez et al., 2014). These results indicated the need to study the genetically modified parasites in depth, including their morphology and *TcCalr* localization. Since an approximate *TcCalr* expression was evaluated by immuno-western blot of epimastigote lysates (Sanchez-Valdez et al., 2013), it is necessary to perform its *in situ* quantification.

Quantification of the gold particles correlated with the genetic modification performed. Thus, the gold-labelled immunoglobulin probes significantly and progressively increased in *TcCalr* +/-, WT and *TcCalr*+ parasites (Fig. 1), facts in agreement with previous results using epimastigote lysates (Sanchez Valdez et al., 2013). An additional

support for the notion that TcCalr is responsible for the parasite virulence and complement resistance observed in previous works is thus provided (Sanchez Valdez et al., 2013; Sanchez-Valdez et al., 2014).

Genetically modified parasites showed altered organelles (Fig. 2D). Their normal elongated shape was lost, in most of the cases. *TcCalr* +/- (Fig. 2A) and *TcCalr*+ (Fig. 2C) epimastigotes had a less defined nucleus and altered structure in some cases. This can be explained, at least in part, by the genetic modification performed. Indeed, both strains, *TcCalr*+ and *TcCalr*+/- present morphologic alterations compared to the WT (Fig. 2D) (See as reference for morphology Fig. 3.) It remains to be determined how the swelling of reservosomes (Fig. 2C) correlates with increased TcCalr expression. It is unlikely that these alterations emerge from a natural polymorphism occurring in the parasites. The life cycle of *T. cruzi* is a continuous process where multiple forms have been described (e.g. spheromastigote) (Tyler and Engman, 2001). The epimastigotes employed in this work were obtained from a cell-free culture, where, the change from epimastigote to amastigote largely depends on the glucose employed in the culture medium (Tyler and Engman, 2001). This also applies to the transition from trypomastigote to epimastigote (Albesa and Eraso, 1981). Whether changes in TcCalr concentration alter the parasite sensitivity to glutaraldehyde and EPON, thus mediating morphological changes, is also a pending issue. Using a Polyclonal antiserum anti-TcCalr (Fig. 4), a direct observation of electron microphotographs showed more TcCalr molecules on the *TcCalr*+ sample (Fig. 4C), as compared to the WT (Fig. 4B) and to the *TcCalr*+/- counterpart (Fig. 4A). In agreement with previous results (Gonzalez et al., 2015) the label was detected mainly in the epimastigote nucleus. Differently from trypomastigotes, perhaps non-infective epimastigotes have a defect that does not allow TcCalr translocation to the parasite surface. However, the label observed was lower as compared to previous results (Gonzalez et al., 2015). This could be explained by the fact that the *T. cruzi* strain used previously (Dm28c) was more virulent (i.e.: expressed more TcCalr) than the one employed in this study, which is an attenuated strain (TCC) (Gonzalez et al., 2015; Sanchez-Valdez et al., 2014). In a previous work (Gonzalez et al., 2015), Dm28c epimastigotes showed less TcCalr molecules in kinetoplast than Dm28c extracellular trypomastigotes or trypomastigotes located inside the host cell. Dm28c epimastigotes had about 22 particles/kinetoplast, while in this work, no more than 6 particles/ $\mu\text{m}^2$  (in the *TcCalr*+ parasite) were detected in the whole TCC epimastigote section used in immunocytochemistry.

The present study could only be performed with epimastigotes, since no genetically modified trypomastigotes could be obtained in a sufficient quantity to perform the electron microscopy studies. Even though some attempts were made to obtain genetically modified trypomastigotes, the *TcCalr*+/- strain was extremely hard to transform, since *TcCalr*+/- epimastigotes had defective metacyclogenesis and the few that successfully transform into trypomastigotes, have their infective capacity diminished, thus not allowing us to obtain the minimum number of parasites required for electron microscopy processing.

## 5. Conclusion

This is the first study that evaluates the morphology of a parasite genetically modified in its capacity to express TcCalr. In agreement with previous functional results, *TcCalr*+/- epimastigotes expressed less TcCalr than WT or *TcCalr*+ epimastigotes *in situ*. Thus, additional studies involving deletions of other genes would be required in order to evaluate the protective immunogenic capabilities of TcCalr hemiallelic trypomastigotes.

## Conflict of interest

The authors, upon submitting this manuscript, do not perceive conflicts of interests.

## Declaration of interest

None.

## Acknowledgements

This work was supported by: FONDECYT- Chile grants 1130099 (AF) and 1151029 (SH); CONICYT-Chile PIA ACT 1402 (SH), ICMP09-015-F-Chile (SH), CORFO-Chile 16CTTS-66390 (SH), DAAD57220037 – Germany (SH) and 57168868-Germany (SH).

## References

- Albesa, I., Eraso, A.J., 1981. Primary isolation of *Trypanosoma cruzi* using hemoculture: effect of media composition on epimastigote differentiation. *Rev. Argent. Microbiol.* 13, 53–58.
- Clayton, J., 2010. Chagas disease: pushing through the pipeline. *Nature* 465, S12–5.
- Ferreira, V., Molina, M.C., Valck, C., Rojas, A., Aguilar, L., Ramirez, G., Schwaeble, W., Ferreira, A., 2004a. Role of calreticulin from parasites in its interaction with vertebrate hosts. *Mol. Immunol.* 40, 1279–1291.
- Ferreira, V., Valck, C., Sanchez, G., Gingras, A., Tzima, S., Molina, M.C., Sim, R., Schwaeble, W., Ferreira, A., 2004b. The classical activation pathway of the human complement system is specifically inhibited by calreticulin from *Trypanosoma cruzi*. *J. Immunol.* 172, 3042–3050.
- Ferreira, V., Molina, M.C., Schwaeble, W., Lemus, D., Ferreira, A., 2005. Does *Trypanosoma cruzi* calreticulin modulate the complement system and angiogenesis? *Trends Parasitol.* 21, 169–174.
- Gonzalez, A., Valck, C., Sanchez, G., Hartel, S., Mansilla, J., Ramirez, G., Fernandez, M.S., Arias, J.L., Galanti, N., Ferreira, A., 2015. *Trypanosoma cruzi* calreticulin topographical variations in parasites infecting murine macrophages. *Am. J. Trop. Med. Hyg.* 92, 887–897.
- Lopez, N.C., Valck, C., Ramirez, G., Rodriguez, M., Ribeiro, C., Orellana, J., Maldonado, I., Albini, A., Anaconda, D., Lemus, D., Aguilar, L., Schwaeble, W., Ferreira, A., 2010. Antiangiogenic and antitumor effects of *Trypanosoma cruzi* Calreticulin. *PLoS Negl. Trop. Dis.* 4, e730.
- Molina, M.C., Ferreira, V., Valck, C., Aguilar, L., Orellana, J., Rojas, A., Ramirez, G., Billetta, R., Schwaeble, W., Lemus, D., Ferreira, A., 2005. An *in vivo* role for *Trypanosoma cruzi* calreticulin in antiangiogenesis. *Mol. Biochem. Parasitol.* 140, 133–140.
- Ramirez, G., Valck, C., Molina, M.C., Ribeiro, C.H., Lopez, N., Sanchez, G., Ferreira, V.P., Billetta, R., Aguilar, L., Maldonado, I., Cattani, P., Schwaeble, W., Ferreira, A., 2011. *Trypanosoma cruzi* calreticulin: a novel virulence factor that binds complement C1 on the parasite surface and promotes infectivity. *Immunobiology* 216, 265–273.
- Ramirez, G., Valck, C., Ferreira, V.P., Lopez, N., Ferreira, A., 2012. Extracellular *Trypanosoma cruzi* calreticulin in the host-parasite interplay. *Trends Parasitol.* 27, 115–122.
- Ramirez-Tolosa, G., Ferreira, A., 2017. *Trypanosoma cruzi* evades the complement system as an efficient strategy to survive in the mammalian host: the specific roles of host/parasite molecules and *Trypanosoma cruzi* calreticulin. *Front. Microbiol.* 8, 1667.
- Ramirez-Tolosa, G., Abello, P., Ferreira, A., 2016. Is the antitumor property of *trypanosoma cruzi* infection mediated by its calreticulin? *Front. Immunol.* 7, 268.
- Sanchez Valdez, F.J., Perez Brandan, C., Zago, M.P., Labriola, C., Ferreira, A., Basombrio, M.A., 2013. *Trypanosoma cruzi* carrying a monoallelic deletion of the calreticulin (TcCRT) gene are susceptible to complement mediated killing and defective in their metacyclogenesis. *Mol. Immunol.* 53, 198–205.
- Sanchez-Valdez, F.J., Perez Brandan, C., Ramirez, G., Uncos, A.D., Zago, M.P., Cimino, R.O., Cardozo, R.M., Marco, J.D., Ferreira, A., Basombrio, M.A., 2014. A monoallelic deletion of the TcCRT gene increases the attenuation of a cultured *Trypanosoma cruzi* strain, protecting against an *in vivo* virulent challenge. *PLoS Negl. Trop. Dis.* 8, e2696.
- Sanchez-Valdez, F.J., Perez Brandan, C., Ferreira, A., Basombrio, M.A., 2015. Gene-deleted live-attenuated *Trypanosoma cruzi* parasites as vaccines to protect against Chagas disease. *Expert Rev. Vaccines* 14, 681–697.
- Sosoniuk, E., Vallejos, G., Kenawy, H., Gaboriaud, C., Thielens, N., Fujita, T., Schwaeble, W., Ferreira, A., Valck, C., 2014. *Trypanosoma cruzi* calreticulin inhibits the complement lectin pathway activation by direct interaction with L-Ficolin. *Mol. Immunol.* 60, 80–85.
- Sosoniuk-Roche, E., Vallejos, G., Aguilar-Guzman, L., Pizarro-Bauerle, J., Weinberger, K., Rosas, C., Valck, C., Michalak, M., Ferreira, A., 2017. Exogenous Calreticulin, incorporated onto non-infective *Trypanosoma cruzi* epimastigotes, promotes their internalization into mammal host cells. *Immunobiology* 222, 529–535.
- Souto-Padron, T., Labriola, C.A., de Souza, W., 2004. Immunocytochemical localisation of calreticulin in *Trypanosoma cruzi*. *Histochem. Cell Biol.* 122, 563–569.
- Tyler, K.M., Engman, D.M., 2001. The life cycle of *Trypanosoma cruzi* revisited. *Int. J. Parasitol.* 31, 472–481.
- Valck, C., Ramirez, G., Lopez, N., Ribeiro, C.H., Maldonado, I., Sanchez, G., Ferreira, V.P., Schwaeble, W., Ferreira, A., 2010. Molecular mechanisms involved in the inactivation of the first component of human complement by *Trypanosoma cruzi* calreticulin. *Mol. Immunol.* 47, 1516–1521.